Sub-Domain Solution of the Boltzmann Equation in MOS Devices by Means of Spherical Harmonics Expansion

A. Pierantoni, M.C. Vecchi and A. Gnudi
Dipartimento di Elettronica, Informatica e Sistemistica
Università di Bologna
Viale Risorgimento 2, 40136, Bologna, ITALY

***Abstract*— A sub-domain solution technique of the Boltzmann Transport Equation (BTE) based on the Spherical Harmonics Expansion (SHE) method is presented, and applied in the channel region of MOSFET's. It is demonstrated that by means of suitable boundary conditions the "exact" solution is well approximated, with an appreciable increase of numerical efficiency.**

I. Introduction

The SHE technique has been demonstrated to be a practical approach for the deterministic solution of the BTE in semiconductors [1],[2],[3]. As opposed to the Monte Carlo method, there is no statistical noise in the high energy tail requiring long computational time, while, on the other hand, the limitations of the approaches based merely on the first moments of the distribution (hydrodynamic or energy transport models) are overcome. The method consists of expanding the distribution function in the momentum space in series of spherical harmonics, replacing such an expansion into the BTE, and solving the resulting system of PDE's in the unknown coefficients of the expansion. The dimensionality of the problem is thus reduced, since the coefficients depend on the real space coordinates $\boldsymbol{r}$ and on the modulus of the momentum k only (or the energy E in the case of spherically symmetric bands). Of course, the method is effective only if the number of terms in the expansion is small. Indeed it has been shown that, by considering only the first two terms of the expansion $f_0(\boldsymbol{r}, E)$ and $f_1(\boldsymbol{r}, E)$, a satisfactory agreement with a full-band Monte Carlo code is obtained, with a substantial reduction of the computational effort [4]. However, in a two-dimensional spatial domain, the size of the discretized system of equations can reach the order of hundreds of thousands of unknowns, due to the energy independent variable that makes the problem effectively three-dimensional. This poses severe problems to the sparse linear system solvers, in terms of both CPU time and memory requirements.

The purpose of this work is to increase the numerical efficiency of the method, by means of a sub-domain solution of the SHE equations, properly coupled with a full hydrodynamic (HD) simulation, in order to get the sub-domain boundary conditions. Similar techniques have been adopted within the Monte Carlo scheme in order to alleviate the problem of the very long simulation times [5],[6],[7]. It will be demonstrated here that a regional solution is a worthwhile method also in the SHE framework.

II. The Spherical-harmonics expansion method

In this section the basic features of the SHE method will be recalled. The distribution function for the electrons in the conduction band is first written, by means of a spherical harmonics series expansion in the momentum space, as [1], [8]

$$f(\boldsymbol{r},\boldsymbol{k}) = f_0(\boldsymbol{r},k) + Y_1{}^n(\theta,\varphi) f_1^n(\boldsymbol{r},k) + Y_2{}^m(\theta,\varphi) f_2^m(\boldsymbol{r},k) + \ldots \qquad n=-1\ldots 1, \quad m=-2\ldots 2 \tag{1}$$

where summation over repeated indices is assumed. In (1), $Y_l{}^m$ are the spherical harmonics functions defined on the unit sphere in the coordinate system (k,θ,φ). By replacing the above expression in the BTE, and matching the coefficients of the terms of equal weight, a system of PDE's in the unknowns $f_1^n(\boldsymbol{r},k)$ and $f_2^m(\boldsymbol{r},k)$ can be worked out. It has been shown that only the terms up to order one can be retained. In addition, by using the coordinate transformation $(\boldsymbol{r},k) \rightarrow (\boldsymbol{r},H)$, where $H = E(k) - q\psi(\boldsymbol{r})$ is the total electron energy and ψ the electrostatic potential, the following system of equations is obtained

$$\frac{\partial}{\partial r_i}\left(g\, u_{\mathrm{g}} f_i\right) + 3\, c_{\mathrm{op}}\, g\, \left(g^+\left[N_{\mathrm{op}}^+ f_0^+ - N_{\mathrm{op}} f_0\right] - g^-\left[N_{\mathrm{op}}^+ f_0 - N_{\mathrm{op}} f_0^-\right]\right) = 0 \tag{2}$$

$$f_i = -\tau_1\, u_{\mathrm{g}}\, \frac{\partial f_0}{\partial r_i} \tag{3}$$

where g is the density of states in the conduction band, u_{g} is the group velocity, c_{op} is a parameter related to the optical phonon coupling constant, N_{op} is the optical phonon occupation number and $N_{\mathrm{op}}^+ = N_{\mathrm{op}} + 1$. The notation $g^\pm = g(H \pm \hbar\omega_{\mathrm{op}})$ has been used, and similarly for $f_0^\pm$, where $\hbar\omega_{\mathrm{op}}$ is the optical phonon energy. The time τ_1 is obtained from a self-consistent expansion of the electron scattering probability $S(k,k')$ through

$$\tau_1^{-1} f_i = f_i \int S_0(k,k')\mathrm{d}^3k' - \frac{1}{3}\int S_1(k',k) f_i(k')\mathrm{d}^3k' \tag{4}$$

The functions f_i are a linear combination of the original coefficients f_1^n of order one. Acoustic, optical phonon,

0-7803-3775-1/97/$10.00 © 1997 IEEE.

ionized-impurity and impact ionization scattering are considered in this work, as well as a pseudo spherical-symmetric band structure which guarantees that the density of states and group velocity are physically correct [4].

Once Eq. (3) has been replaced into Eq. (2), a second order difference-differential equation is obtained in the unknown f_0. Conditions are required for f_0 at the geometrical boundaries (Dirichelet conditions at the ohmic contacts, and Neumann conditions at the free boundaries and at the silicon-oxide interface are normally prescribed), while at the energy extrema ($E = 0$ and $E = E_{max}$) it is sufficient to look for a regular solution. One of the objectives of this work is to find suitable conditions at the sub-domain boundaries.

III. The window solution technique

The proposed window solution method works as follows.

1. A HD simulation is performed on the full device, in order to obtain the electric potential ψ, the electron concentration n and the electron temperature T_n. The transport parameters of the HD model, such as the mobility and the energy relaxation time, have been calibrated in accordance with the scattering rates and the full-band structure of the BTE, by means of spatially uniform simulations.

2. A rectangular sub-domain (window) is selected in the regions where the high energy distribution is required. In a MOSFET such a window should necessarily include the hot spot at the drain end of the channel. The size and location of a typical window is illustrated in Fig. 1.

3. The SHE equations are solved only in the selected window, using the potential previously calculated from the HD solution, and by means of suitable boundary conditions that try to match the outer solution.

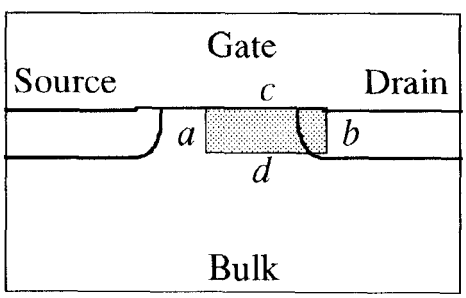

Fig. 1. Typical sub-domain for a MOSFET

We have experimented with windows of different sizes, some of which are indicated in the inner spot of Figures 4, 5 and 6. With reference to the general case of Fig. 1, Neumann conditions are assumed at the silicon-oxide interface (side c) and also at the bulk side (d), where the latter choice is motivated by the side d being well inside the depletion region. Boundaries a and b have been treated in different ways.

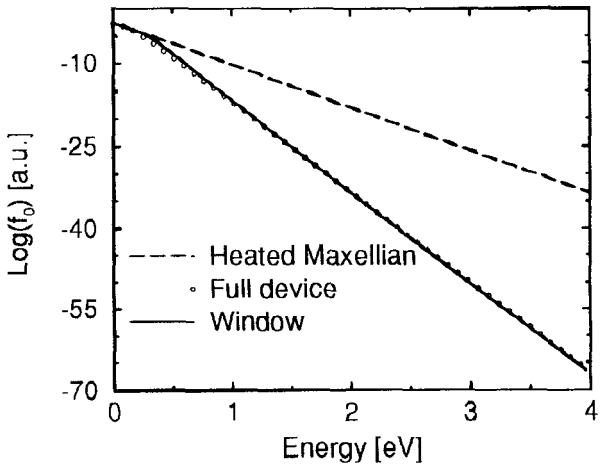

Fig. 2. Boundary distribution at the side a

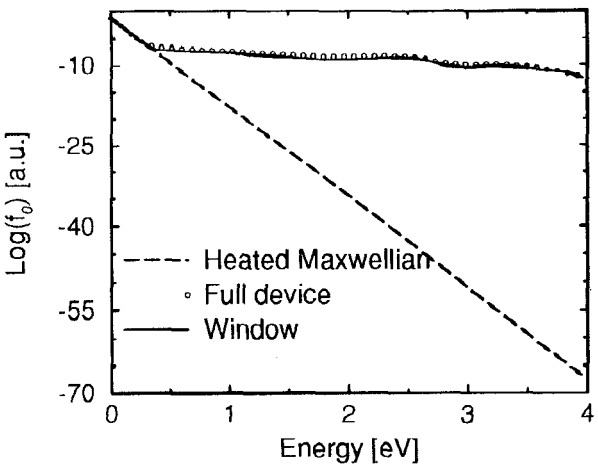

Fig. 3. Boundary distribution at the side b

The simplest choice is to force the equilibrium distribution pointwise along sides a and b

$$f_0(n,E)_{eq} \equiv n \frac{\exp(-E/K_B T_0)}{\int g(E)\exp(-E/K_B T_0)\mathrm{d}E} \tag{5}$$

where T_0 is the lattice temperature. This condition obviously works well when the window extends well inside the source and drain neutral regions, where thermal equilibrium is nearly verified. However, in order to increase the numerical efficiency, the use of a smaller window, possibly localized at the drain end of the channel, would be preferable.

The next degree of approximation is to assume on sides a and b a heated Maxwellian distribution

$$f_0(n,E)_{hm} \equiv n \frac{\exp(-E/K_B T_n)}{\int g(E)\exp(-E/K_B T_n)\mathrm{d}E} \tag{6}$$

This function turns out to be a good approximation of the "real" distribution only at very low energies, while it is far off at high energies. This is clearly shown in Figs. 2 and 3, where $f_0(n,E)_{hm}$ (label "heated maxwellian") and the real distribution obtained from the complete SHE solution (label "full device"), are compared, at the two corners between the silicon surface and the sides a and b respectively. In Fig. 2 (source side), electrons with energy above 0.3 eV are still distributed in accordance with an exponential

equilibrium slope ("full device"), whereas in Fig. 3 (just inside the drain), the low part of the distribution is dominated by the cold electrons residing in the drain, with a tail of hot electrons coming from the channel which is completely ignored by the description based on the HD temperature. For increasing the accuracy, new boundary conditions have been introduced, referred to by the label "window" in all the figures. At the outflow boundary, we have generalized the method proposed in [9] for the metal-semiconductor interfaces. Starting from the particle conservation equation

$$f_{out}(\boldsymbol{k}_{out})\,\boldsymbol{u}_{out}\cdot\hat{\boldsymbol{n}}\,\mathrm{d}^3k_{out} = f_{in}(\boldsymbol{k}_{in})\,\boldsymbol{u}_{in}\cdot\hat{\boldsymbol{n}}\,\mathrm{d}^3k_{in} \qquad (7)$$

applied at the side b, where the subscripts "*out*" and "*in*" stand for the outer and the inner region with respect to the selected window, and $\hat{\boldsymbol{n}}$ is the unit vector normal to the same side b, and applying the spherical harmonics expansion, the following equation is obtained

$$f_{0,out} = f_{0,in} + \frac{2}{3}\tau_1 u_g \frac{\partial f_{0,in}}{\partial r_n} \qquad (8)$$

where r_n is the normal direction to the boundary. Eq. (8) can be considered a mixed boundary condition for the unknown $f_{0,in}$, which must be solved together with the system equations. For $f_{0,out}$ we use the expression of $f_o(n,E)_{hm}$ given in Eq. (6). As shown in Fig. 3 (label "window"), this approach gives the correct energy tail at the outflow boundary. Unfortunately, it can not be applied at the inflow side. However, as already observed, from the curve labelled "full device" in Fig. 2 (side *a*) it is seen that the distribution exhibits an equilibrium exponential decay at high energy. This suggests to define the boundary condition there by means of an exponential function with two different slopes, one related to T_n at low energies, and the other one to T_0 at high energies. Two additional parameters are required, the break energy and the normalization n-dependent factor, which are calculated by imposing the HD mean energy and concentration. Such a distribution is shown in Fig. 2 with the label "window".

IV. Simulation Results

The proposed method has been tested on three different devices: a FLASH-EEPROM of $0.9\mu m$ channel length, a $0.5\mu m$ standard MOSFET, and a $0.2\mu m$ LDD MOSFET. The full device geometries and the sub-domains are sketched in Figs. 4, 5 and 6, together with the corresponding bulk currents due to impact ionization, as functions of the gate voltage. The label "window" refers to the sub-domain solution with the use of the boundary conditions described in the previous section. The two curves are very close, while the CPU time and memory saving is larger than a factor two. It should be noticed that we have used highly flexible triangular grids particularly well refined in the channel, with an average number of 3000 nodes, while the average window contains almost 1500 nodes. The computational advantage would be much larger if a more uniformly spaced grid were used.

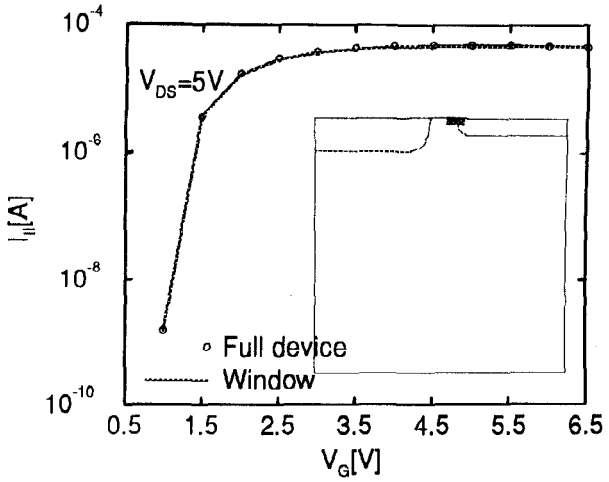

Fig. 4. Comparison of the bulk currents in the EEPROM

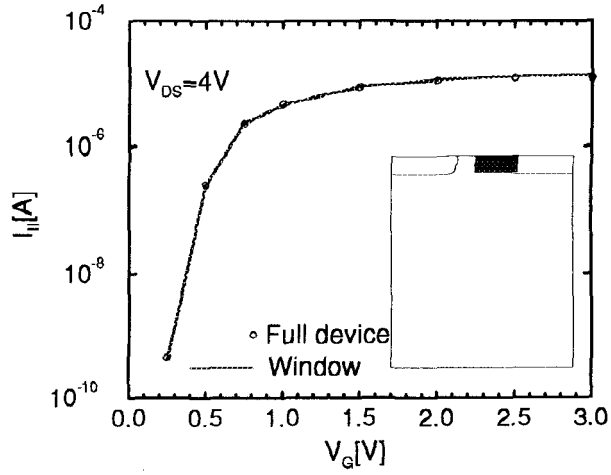

Fig. 5. Comparison of the bulk currents in the MOSFET

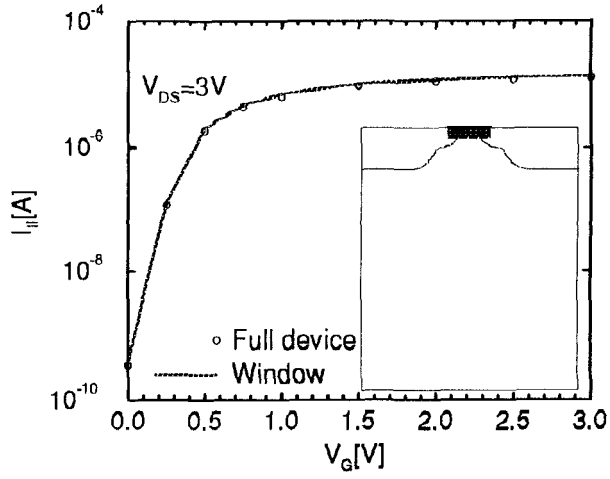

Fig. 6. Comparison of the bulk currents in the LDD MOSFET

The electron concentration and temperature at the interface in the channel for a particular bias point of the MOSFET is reported in Fig. 7, with the window extending from $length = 0.5\,\mu$m to $length = 0.72\,\mu$m. Fig. 8 shows the distribution function in a point in the channel corresponding to the region where the temperature starts to decay toward the drain ($length \simeq 0.66\,\mu$m in Fig. 7). The "window" solution agrees well with the "full device" solution up to 4 eV.

In Fig. 9 the two solutions are compared at all the points at the interface of the EEPROM cell. It can be seen that the error at high energies due to the imprecise boundary condition at the source side (length=2.06 μm) tends to decrease towards the drain, and practically vanishes in the hot spot (length=2.27 μm). The results of Figs. 8 and 9 suggest that the presented technique could also help in the calculation of the oxide injection current.

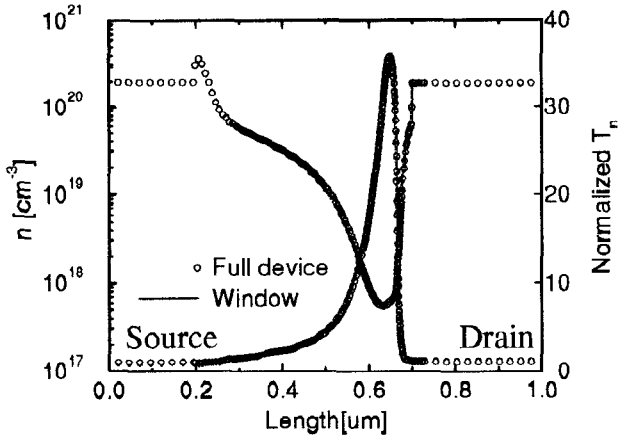

Fig. 7. Electron temperature and concentration profiles at the interface of the MOSFET

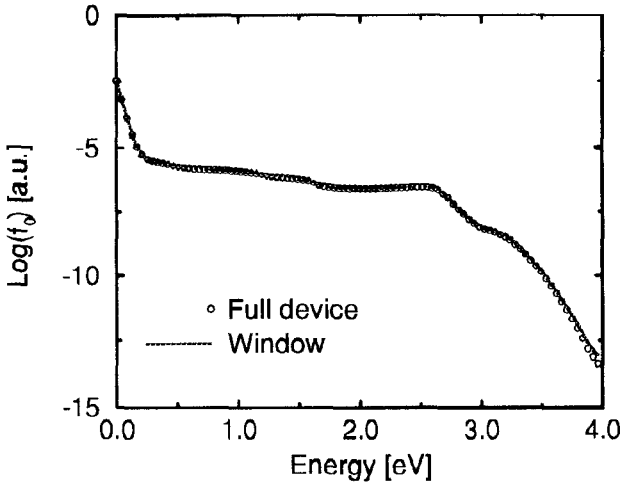

Fig. 8. Distribution function at section *length* $\simeq 0.66\mu$m of Fig. 7

V. Conclusion

A "window" solution of the SHE method of the BTE has been presented, which, in combination with suitable regional boundary conditions, has been demonstrated to lead to high energy electron distributions and impact ionization bulk currents in good agreement with the results of a full device simulation in MOSFET like devices. The window typically covers the portion of the channel where the electron temperature significantly departs from equilibrium. The increase of numerical efficiency is of the order of more than a factor two. In perspective, the method could be completed with a partially automatic procedure for the selection of the sub-domain, and used mainly for the calculation of the oxide injection current.

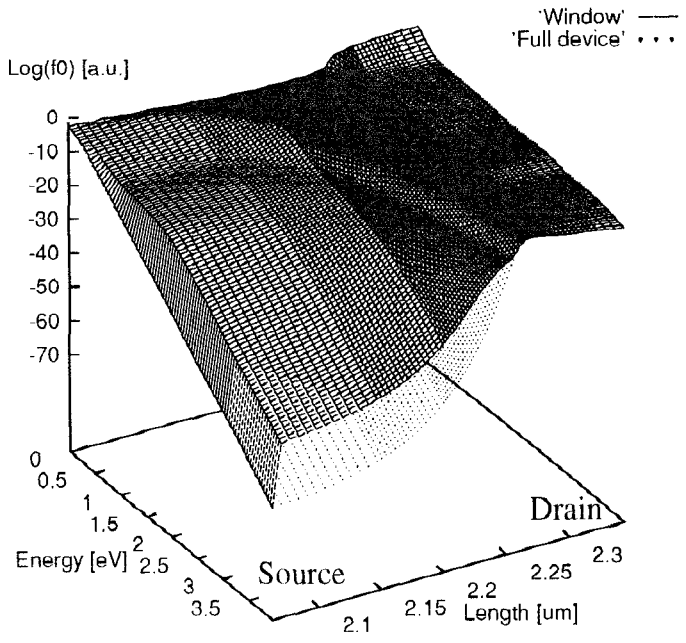

Fig. 9. Distribution function at the channel interface of the EEPROM

Acknowledgment

Access to ISE Integrated Systems Engineering AG software for Hydrodynamic simulations is acknowledged.

References

[1] A. Gnudi., D. Ventura, and G. Baccarani, "Two-dimensional MOSFET simulation by means of a multidimensional spherical harmonics expansion of the Boltzmann transport equation," *Solid State Electronics*, vol. 36, pp. 575–581, 1993.

[2] K.A. Hennacy, Y.J. Wu, and N. Goldsman, "Deterministic MOSFET simulation using a generalized spherical harmonics expansion of the Boltzmann equation," *Solid State Electronics*, vol. 38, pp. 1485–1495, 1995.

[3] K. Rahmat, J. White, and D.A. Antoniadis, "Simulation of semiconductor devices usic Galerkin/spherical harmonics expansion approach to solving the coupled Poisson-Boltzmann equation," *IEEE Trans. on CAD*, vol. 15, pp. 1181–1196, 1996.

[4] M. C. Vecchi, A. Pierantoni, A. Greiner, and M. Rudan, "Modeling of surface-scattering mechanisms and soft-threshold impact-ionization in the analysis of realistic MOS devices," in *Proceedings of the Sixth ULSI Science and Technology Conference*, 1997, pp. 601–612.

[5] D.Y. Cheng, C.G. Hwang, and R.W. Dutton, "PISCES-MC: a multimethod 2-D device simulator," *IEEE Trans. on CAD*, vol. 7, pp. 1017–1026, 1988.

[6] H. Kosina and S. Selberherr, "A hybrid device simulator that combines Monte Carlo and Drift-Diffusion analysis," *IEEE Trans. on CAD*, vol. 13, pp. 201–210, 1994.

[7] U. Krumbein, P.D. Yoder, A. Benvenuti, A. Shenk, and W. Fichtner, "Full-band Monte Carlo transport calculation in a integrated simulation platform," in *Proceedings of the Sixth SISDEP Conference*, 1995, pp. 400–403.

[8] D. Ventura, A. Gnudi, and G. Baccarani, "Multidimensional spherical harmonics expansion of Boltzmann equation for transport in semiconductors," *Applied Mathematics Letters*, vol. 5, no. 3, pp. 85–90, 1992.

[9] D. Schroeder, D. Ventura, A. Gnudi, and G. Baccarani, "Boundary conditions for spherical harmonics expansion of Boltzmann equation," *Electronics Letters*, vol. 28, pp. 995–996, 1992.